






BCI System using a Novel Processing Technique Based on Electrodes Selection for Hand Prosthesis Control^{*}

Alisson Constantine  * Víctor Asanza  *
Francis R. Loayza  ** Enrique Peláez  *
Diego Peluffo-Ordóñez  ***,****,†

* *Facultad de Ingeniería en Electricidad y Computación, Escuela Superior Politécnica del Litoral, ESPOL, Campus Gustavo Galindo km 30.5 Vía Perimetral, P.O. Box 09-01-5863, Guayaquil, Ecuador (e-mail: {alasccons,vasanza,epelaez}@espol.edu.ec)*

** *Facultad de Ingeniería en Mecánica y Ciencias de la Producción, Escuela Superior Politécnica del Litoral, ESPOL, Neuroimaging and Bioengineering Laboratory, LNB, Campus Gustavo Galindo km 30.5 Vía Perimetral, P.O. Box 09-01-5863, Guayaquil, Ecuador (e-mail: floayza@espol.edu.ec)*

*** *Smart Data Analysis Systems Group (SDAS Research Group - www.sdas-group.com), Ben Guerir 47963, Morocco (e-mail: {diego.peluffo}@sdas-group.com)*

**** *Modeling, Simulation and Data Analysis (MSDA) Research Program, Mohammed VI Polytechnic University, Ben Guerir 47963, Morocco (e-mail: peluffo.diego@um6p.ma)*

† *Faculty of Engineering, Corporación Universitaria Autónoma de Nariño, Carrera 28 No. 19-24, Pasto, Colombia, 520001, (email: diego.peluffo@aunar.edu.co)*

Abstract:

This work proposes an end-to-end model architecture, from feature extraction to classification using an Artificial Neural Network. The feature extraction process starts from an initial set of signals acquired by electrodes of a Brain-Computer Interface (BCI). The proposed architecture includes the design and implementation of a functional six Degree-of-Freedom (DOF) prosthetic hand. A Field Programmable Gate Array (FPGA) translates electroencephalography (EEG) signals into movements in the prosthesis. We also propose a new technique for selecting and grouping electrodes, which is related to the motor intentions of the subject. We analyzed and predicted two imaginary motor-intention tasks: opening and closing both fists and flexing and extending both feet. The model implemented with the proposed architecture showed an accuracy of 93.7% and a classification time of 8.8 μ s for the FPGA. These results present the feasibility to carry out BCI using machine learning techniques implemented in a FPGA card.

Keywords: Bio-signals analysis, Neural Networks, Brain Computer Interface, Embedded Systems, FPGA

1. INTRODUCTION

An essential part of the body, the human hand performs precise, heavy, and fast operations, using 27 degrees of freedom for all its movements. Today, millions of people suffer from limb loss due to amputations, which causes a significant effect on their life (McDonald et al., 2020).

The human hand is controlled by neuron action potentials that stimulate muscle contraction to produce joint movements. The neural stimuli travel from the brain to the muscles through motor neurons located in the spinal cord. These stimuli come from the conjunction of different parts

of the brain, as detailed by the Penfield Homunculus (Roux et al., 2018) and Brodmann's areas of the cerebral cortex (Zilles, 2018). The neural activity generated in these brain regions while performing a task can be detected, measured, recorded, and filtered to control an artificial mechanism.

Access to these stimuli could be difficult, as described in (Osborn et al., 2018). Capturing these signals directly from the nerves requires invasive methods. However, they can be recorded using minimally invasive procedures, as proposed by (Petrini et al., 2019). One of the non-invasive techniques is using electromyography (EMG) (Zhang et al., 2018) or EEG (Parr et al., 2019) to record the activity that naturally accompanies hand movements.

* Escuela Superior Politécnica del Litoral, ESPOL.

1.1 Related Work

Today, EEG has a great impact on the development of assistive rehabilitation devices and prostheses. The integration of Artificial Intelligence (AI) techniques into the analysis of EEG signals facilitates the autonomous classification or interpretation of a subject's intention (Asanza et al., 2020, 2018). Additionally, its low cost, compatibility with other devices, portability, and high temporal resolution, make capturing EEG signals one of the most suitable approaches for analyzing neuron action potentials through BCIs (Becerra et al., 2019).

For active prosthesis control, (Cedeño Z. et al., 2019) used EMG sensors to detect motor intentions with 95% of accuracy. However, these sensors require residual motor activity from the subject. Recent work uses EEG recorded from the prefrontal cortex for actively controlling hand prostheses (Fuentes-Gonzalez et al., 2021). This method requires that the test subject concentrates or relaxes to generate β or α cerebral waves.

In this paper, we use EEG data recorded during an experiment on the motor cortex area (Goldberger et al., 2000). The data was collected while performing motor and imaginary tasks. We preprocessed the data to eliminate noise components. For predicting the imaginary motor intention of the subjects, we designed an end-to-end model architecture. Feature extraction is performed on signals acquired through EEG recording. We use an Artificial Neural Network for classification. The proposed architecture includes a control stage based on an FPGA that translates intentions into movements for the robotic hand (Armijos et al., 2020).

This paper is structured as follows: Section II describes the materials and methods used for acquiring and preprocessing data; section III shows the results from the experiments with the proposed methodology. Finally, in section IV, we draw some conclusions and make suggestions for future work.

2. MATERIALS AND METHODS

The methodology has six stages: Design of a 3D-printed hand, data acquisition, preprocessing, feature extraction, classification, and control of the 3D device.

2.1 The EEG Dataset

The EEG dataset used for training the model comes from the PhysioNet free database (Goldberger et al., 2000). The data was acquired using a 64 channel electroencephalograph with surface electrodes following the international 10-20 system. Goldberger et al. (Goldberger et al., 2000) recorded the signals using the BCI2000 system (Schalk et al., 2004), with a sampling frequency of 160Hz.

Subjects randomly performed each movement for 4.1 seconds, using one-second intervals to complete a total of 90 repetitions. During the test, a target appears at the top or the bottom of a screen. If it appears at the top, the subject imagines opening and closing both fists; if it appears at the bottom, the subject imagines flexing and extending both feet. We refer to these actions as Movements 1 and 2 (M1

and M2), respectively. The participant concentrates until the target disappears, then relaxes.

2.2 Hardware implementation

A 3D printed hand was designed and created, following the guidelines as defined by (Fuentes-Gonzalez et al., 2021), with some modifications done using a free and open source 3D creation suite (Blender), which allowed us to include an additional DOF to the thumb finger; this modification included the option of using rotary servo-motors instead of linear servo-motors. The created hand has 6 DOF in total, 2 for the thumb and one for the rest of the fingers. For each DOF, a micro servo-motor model SG90 was used, attached to a sleeve at each finger joint, The final model is shown in Figure 1.

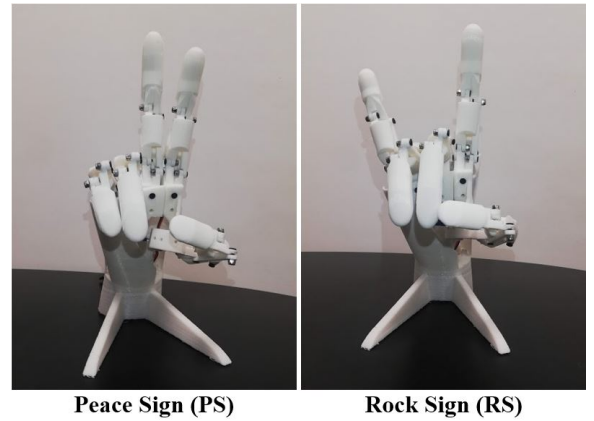


Fig. 1. 3D printed hand and programmed movements in the robotic hand related to M1 and M2 motor intentions described in section 2.3

We use a NIOS II/e processor as a controller and implement it in an Altera Cyclone® V FPGA on a DE0-Nano-SoC (System on a Chip) board. Figure 2 shows the architecture of the controller. In this configuration, the EEG data from each electrode is sent through a UART (Universal Asynchronous Receiver-Transmitter) communication circuit to the ARM (Advanced RISC Machines) processor of the card via the AXI (Advanced eXtensible Interface) bus. We use the ARM processor to compute the predictions of the motor intentions. The ARM processor activates the GPIO (General-Purpose Input/Output) pins corresponding to each servo-motor of the robotic hand. The AXI bus communicates with the AVALON bus through the IIPS-FPGA interfaces. Via the AXI bus, the PWM (Pulse-width Modulation) controllers communicate with the GPIOs of the FPGA, available in the card.

The hand connects with the GPIO pins of the FPGA through a servo-motor control card. The card is designed to have an orderly plug-and-play distribution of the servo-motors that can be selected using jumpers. This feature allows selecting the power supply of the servo-motors, either from the FPGA or from an external 5 Vdc source.

2.3 System Structure

We designed a non-invasive offline with the downloaded data, using a BCI strategy, as shown in Figure 3. In

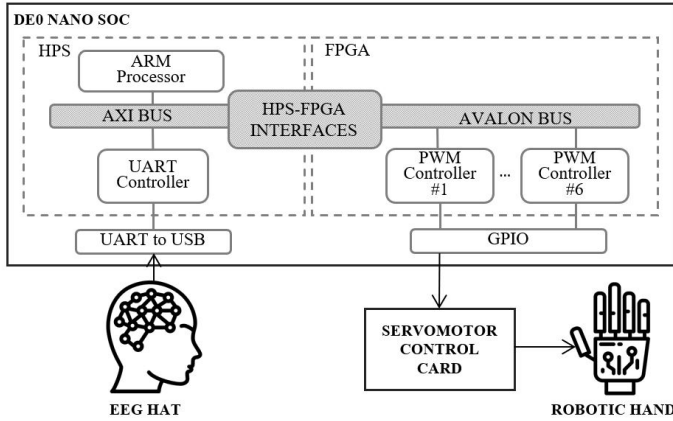


Fig. 2. Description of the SoC used for the interconnection of the hardware elements.

this configuration, data were acquired from 10 healthy volunteers, as described in section 2.1.

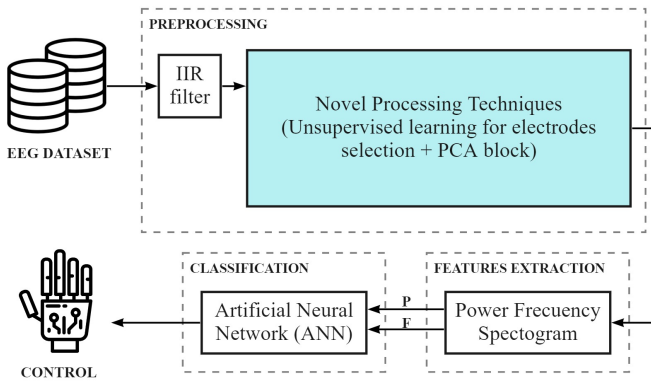


Fig. 3. Structure of the online approach BCI system

From the movements used to control the hand, M1 was used to perform the Peace Sign (PS) and M2 for the Rock Sign (RS), as shown in Figure 1. After that, each movement was saved following the European EDF format. Each task had a total of 656 samples, and for each subject, there were 46 files, 23 corresponding to PS and 23 to RS.

2.4 Data Preprocessing

Once the EEG signals have been acquired, it is necessary to perform preprocessing to maximize relevant information embedded in the EEG samples. Additionally, preprocessing isolates the signals associated with particular brain activity, during a specific period within a given frequency range (Bansal and Mahajan, 2019). To achieve this extraction, to be able to segment the continuous EEG data, and for selecting the significant signals captured from the electrodes, which will be used for training the machine learning model, we used the diagram shown in Figure 4.

Infinite Impulse Response filter (IIR). As (Bansal and Mahajan, 2019) pointed out, when dealing with imaginary motor tasks, the bands related to EEG data of interest are reflected in the α , μ , and β bands. Hence, we designed temporal filters to select specific EEG subfrequencies. We implement a Butterworth order 162 double-pass digital IIR filter with a bandpass from 8 to 31 Hz using Matlab 2016.

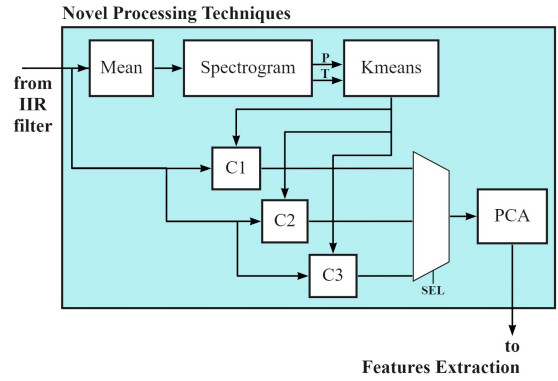


Fig. 4. Unsupervised learning architecture for selecting the electrodes and significant signals with PCA.

Statistical mean. For each and every movement we evaluated the statistical mean, i.e. the average of all corresponding signals in the N files. The signals were captured from each electrode at each sampled time, generated a single file containing the RMS values of all files of the same movement.

Spectrogram. The EGG signals have particular properties such as non-linearity, non-Gaussian and non-stationary. Hence, to focus on their frequency with non-linear characteristics, as well as on their temporal linear characteristics, we applied a Short-Term Fourier Transform (STFT) to each task executed during 4.1s (656 samples). As a result, three characteristics were extracted: Power, frequency, and time of the signal as shown in Figure 5.

3D Spectrogram

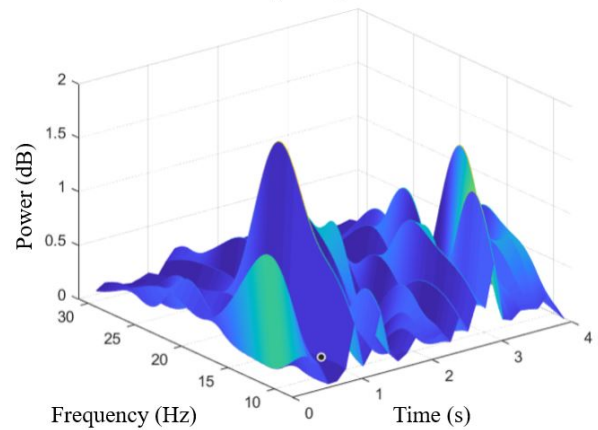


Fig. 5. 3D Spectrogram of each of the tasks executed during 4.1s (656 samples).

With the combination of these signals, we created a Power Time (PT) that represents the RMS values of time versus power at all time instant for each of the 64 electrodes. The electrodes are synchronized in time and contribute information at the time the subject performs a motor activity.

Hybrid K-means Clustering. As described before, when acquiring EEG signals, it is necessary to select the electrodes that better perform during this process due to the presence of interferences. Data captured through these

electrodes is later used to analyze specific signals related to the neurophysiological activity of interest. Then, this data is clustered into K groups by their similarity within the group, as well as their dissimilarity between elements of different groups (Sinaga and Yang, 2020). To choose the appropriate number of groups into which the signal should be divided, we used the Calinski-Harabaz criterion, which is determined by (1):

$$CH(k) = \frac{B_c(k)}{k-1} / \frac{W_c(k)}{n-1} \quad (1)$$

Where n represents the number of elements in a cluster and k the number of clusters. B_c denote the quadratic sum of the distance between the elements inside a cluster, and W_c the quadratic sum of the distance between the elements outside a cluster.

The criteria determined in (1) let us analyze each possible solution of the clusters based on their quality. This feature determines how large the inter-cluster distances are and the proximity to the intra-cluster data (Zaki and Meira, 2014). In this case, the optimal number of clusters determined was three.

For clustering the pre-processed data, we used an unsupervised K-means algorithm. Once it was applied, we validated the electrodes of each group using the Silhouette coefficient (Režanková, 2018). After applying k-means, and validating the groups, we obtained the saved signals after applying the temporary filter of the electrodes corresponding to each group saved in different files.

Principal Component Analysis (PCA). To focus on the features that better capture the neurophysiological responses from the subjects executing a task, a dimensionality reduction such as PCA has been used (Artoni et al., 2018). To select the number of PCs to use, we select the smallest number of dimensions so that the subspace covered by those dimensions captures at least 99% of the total variance (Zaki and Meira, 2014). Based on the statistical analysis of the dataset used in this research, four PCs for each of the tasks performed by the subjects, allowed us to maintain 99% of the information, and at the same time, reducing the need for expensive computational resources necessary to perform the features' extraction task, based only on those PCs.

2.5 Features extraction

We extracted the Frequency Power spectrum of the signals, as well as the RMS values of the principal components of each event belonging to each group obtained in K-means using Spectrogram. The values extracted were stored in a vector indexed by columns, resulting in a matrix of 4096 columns and n rows for each task, where n is the number of electrodes selected by K-means depending on the task.

2.6 Classification

For the classification stage we used a supervised learning strategy, based on a MLP Neural Network (Svozil et al., 1997). We performed the training using Stochastic Gradient Descend (SGD) and the updating of parameters

through Backpropagation. The MLP was designed as a 3 layer full neural network; the input layer was configured with 4096 neurons, corresponding to the size of the input vector; the output layer, contains 2 neurons, based on the number of tasks to be classified. The hidden layer contains 10 neurons for the best configuration, as described in section III. Each neuron was configured to respond to the incoming signals, based on the sigmoid activation function, as detailed in (2):

$$\phi(z) = \frac{1}{1 + e^{-z}}. \quad (2)$$

The training process lasted until the accuracy was higher than 90%; therefore, after the network was trained and validated, and reached the expected accuracy and loss, its architecture was implemented in C++, and its respective learned weight matrix. The threshold coefficients, and other parameters were also embedded into the FPGA-based system.

2.7 Control

As defined, the architecture of our model ends with a control, which interfaces with the BCI. The control structure is detailed in Algorithm 1.

Algorithm 1 Robotic Hand Movement Algorithm

Result: Movement of Robotic Hand

Init: Begin button is press;

```

while Always do
  Read pre-processed EEG data and send it to the Neural
  Network;
  if M1 predicted then
    | PS Sign;
  else
    if M2 predicted then
      | RS Sign;
    else
      | Initial Hand position;
    end
  end
end

```

3. RESULTS AND ANALYSIS

As it is shown in figure 6, the K-means algorithm identified 3 clusters that represent the number of groups of electrodes that better captured the neurophysiological responses. The number of electrodes belonging to each group depends on the movement made by the subject. As we can see, for the case of electrode 13, the K-means algorithm identified it as a group in itself, which is far from the rest of the clusters. Therefore, this cluster was not considered in this analysis. The signal belonging to this group showed a lot of noise during their acquisition process and there might be several reasons why this could be happening, from a damage electrode to a loose connection that compromises the data capture process at this electrode.

The groups used in the analysis are C1 and C3 for PS, and C1 and C2 for RS, as shown in figure 6. The clusters of electrodes for the PS and RS movements are well

identified and differentiated from each other, and there are not data points located in a different cluster. The results obtained by the Silhouette coefficient confirmed that the electrodes were well grouped and none were eliminated for the classification stage.

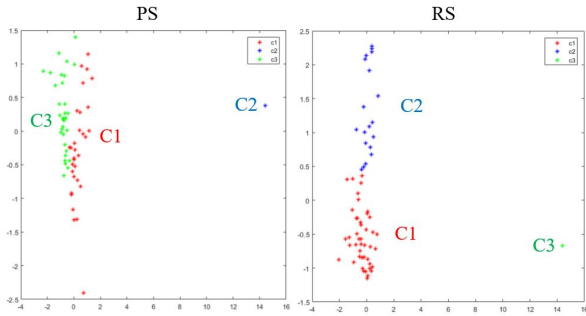


Fig. 6. Cluster Assignments and Centroids for PS and Rs signs.

For the MLP training process the dataset was fragmented as follows: 70% of the dataset was randomly chosen for training; 15% was used for validation during training, and the remaining 15% of the dataset was used for testing purposes.

In the classification stage, we obtained better results for groups C3 of PS and C2 of RS. We trained the MLP using different configurations for the hidden layer. We use an increasing number of neurons, such as 5, 10, 15, 20, and 30 neurons, until we got an acceptable performance of the MLP architecture for the FPGA without affecting the response time. For these configurations the results were: 94.8%, 96.4%, 94.3%, 92.4%, and 90.5% respectively.

After the best performance was obtained with ten neurons in the hidden layer, we tested the MLP with 63 new data points that make up the remaining 15% of the dataset not used during training nor validation. The confusion matrix in Figure 7 shows the best performance in this configuration.

10HL Test Confusion Matrix			
Output Class	30 47.6%	2 3.2%	93.8% 6.3%
	2 3.2%	29 46.0%	93.5% 6.5%
	93.8% 6.3%	93.5% 6.5%	93.7% 6.3%

Fig. 7. Test Confusion Matrix.

In this confusion matrix, each column of the matrix represents the number of predictions for each class, in our case, PS and RS. Meanwhile, each row represents the instances in the real class, allowing us to see what types of successes and errors our model is having during the learning process. In this case, 30 out of the 32 data points belonging to the PS event were classified by the MLP as

PS and 2 as RS; 29 out of the 31 elements belonging to the RS class were classified as RS, and 2 as PS, which represents an accuracy of 93.7%.

Once this MLP neural network has complied with our expected performance, and before translating this architecture to the FPGA, we verified and validated the results of the confusion matrix using 60 new data points. As a result, we achieve an average precision of 95.1%, hence, this network configuration was used with the BCI.

Figure 8 shows that for the PS and RS signals associated with the M1 and M2 movements there were 32 and 19 electrodes used, respectively. The figure represents the selected electrodes that provide significant information in the classification for each imaginary task. The location of these electrodes allowed us to determine the areas of the cerebral cortex that were involved in executing these tasks.

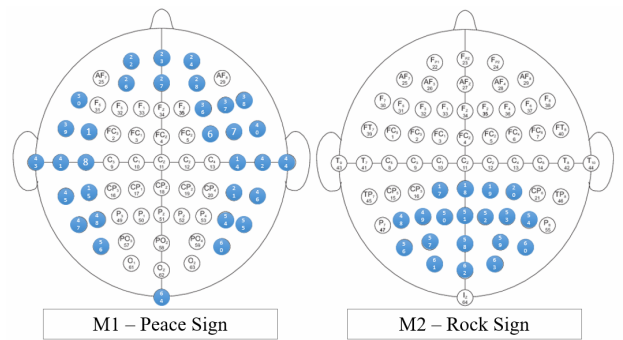


Fig. 8. Electrodes used in the M1 and M2 motor intention.

The DE0-Nano-SoC development card has 40K logic elements that can be controlled by software. Table 1 shows a summary of the resources used in this implementation. We can see that 52% of the logic elements have been used, as well as 73% of the total number of pins. Thus, it is possible to continue using more of its resources such as the embedded PWM blocks to control more servo motors and embedded communication protocol blocks, among others.

Table 1. Resources Used by the FPGA

Resources	Utilization
Logic utilization (in ALMS)	9328/15880 (52%)
Total block memory bits	2048/2764800 (< 1%)
Total pins	230/314 (73%)

4. CONCLUSIONS

We observe that the location of the electrodes for each task concur with the location of the extremities in the Penfield Homunculus: for M1, the electrodes are concentrated at the end of the motor and somatosensory cortex; for M2, in the central part of the brain. The location also matches the Brodmann Areas for imaginary motor movement and imaginary visual tasks.

Classification based on signals captured through the electrodes that are correlated in time is possible. The proposed classification model allowed the interpretation of the imaginary movements of the subject with an accuracy of 93.7%, which then will be translated to the prosthetic hand.

The processing time and the total amount of resources used in the FPGA are optimal enough to execute the MLP neural network and classify the data in about 8.8 μ s.

ACKNOWLEDGMENTS

The authors are greatly grateful by the support given by the SDAS Research Group (www.sdas-group.com) as well as the internal editor J. Mejía-Ordóñez for the manuscript reviewing and editing.

REFERENCES

- Armijos, V.A., Chan, N.S., Saquicela, R., and Lopez, L.M. (2020). Monitoring of system memory usage embedded in fpga. In *2020 International Conference on Applied Electronics (AE)*, 1–4. doi:10.23919/AE49394.2020.9232863.
- Artoni, F., Delorme, A., and Makeig, S. (2018). Applying dimension reduction to EEG data by principal component analysis reduces the quality of its subsequent independent component decomposition. *NeuroImage*, 175, 176–187. doi:10.1016/j.neuroimage.2018.03.016.
- Asanza, V., Constantine, A., Valarezo, S., and Peláez, E. (2020). Implementation of a classification system of eeg signals based on fpga. In *2020 Seventh International Conference on eDemocracy eGovernment (ICEDEG)*, 87–92. doi:10.1109/ICEDEG48599.2020.9096752.
- Asanza, V., Peláez, E., Loayza, F., Mesa, I., Díaz, J., and Valarezo, E. (2018). Emg signal processing with clustering algorithms for motor gesture tasks. In *2018 IEEE Third Ecuador Technical Chapters Meeting (ETCM)*, 1–6. doi:10.1109/ETCM.2018.8580270.
- Bansal, D. and Mahajan, R. (2019). Chapter 2 - eeg-based brain-computer interfacing (bci). In *EEG-Based Brain-Computer Interfaces*, 21–71. Academic Press. doi: <https://doi.org/10.1016/B978-0-12-814687-3.00002-8>.
- Becerra, M.A., Londoño-Delgado, E., Botero-Henao, O.I., Marín-Castrillón, D., Mejia-Arboleda, C., and Peluffo-Ordóñez, D.H. (2019). *Lecture Notes in Computer Science (including subseries Lecture Notes in Artificial Intelligence and Lecture Notes in Bioinformatics)*, volume 11466 LNBI, inbook Low Resolution Electroencephalographic-Signals-Driven Semantic Retrieval: Preliminary Results, 333–342. Springer Verlag.
- Cedeño Z., C., Cordova-Garcia, J., Asanza A., V., Ponguillo, R., and Muñoz M., L. (2019). k-nn-based emg recognition for gestures communication with limited hardware resources. In *2019 IEEE SmartWorld, Ubiquitous Intelligence Computing, Advanced Trusted Computing, Scalable Computing Communications, Cloud Big Data Computing, Internet of People and Smart City Innovation (SmartWorld/SCALCOM/UIC/ATC/CBDCOM/IOP/SCI)*, 812–817. doi:10.1109/SmartWorld-UIC-ATC-SCALCOM-IOP-SCI.2019.00170.
- Fuentes-Gonzalez, J., Infante-Alarcón, A., Asanza, V., and Loayza, F.R. (2021). A 3d-printed eeg based prosthetic arm. In *2020 IEEE International Conference on E-health Networking, Application Services (HEALTHCOM)*, 1–5. doi:10.1109/HEALTHCOM49281.2021.9399035.
- Goldberger, A.L., Amaral, L.A.N., Glass, L., Hausdorff, J.M., Ivanov, P.C., Mark, R.G., Mietus, J.E., Moody, G.B., Peng, C.K., and Stanley, H.E. (2000). PhysioBank, PhysioToolkit, and PhysioNet. *Circulation*, 101(23). doi:10.1161/01.cir.101.23.e215.
- McDonald, C.L., Westcott-McCoy, S., Weaver, M.R., Haagsma, J., and Kartin, D. (2020). Global prevalence of traumatic non-fatal limb amputation. *Prosthetics and Orthotics International*, 0(0), 0309364620972258. doi:10.1177/0309364620972258.
- Osborn, L.E., Dragomir, A., Betthausen, J.L., Hunt, C.L., Nguyen, H.H., Kaliki, R.R., and Thakor, N.V. (2018). Prosthesis with neuromorphic multilayered e-dermis perceives touch and pain. *Science Robotics*, 3(19), eaat3818. doi:10.1126/scirobotics.aat3818.
- Parr, J.V.V., Vine, S.J., Wilson, M.R., Harrison, N.R., and Wood, G. (2019). Visual attention, EEG alpha power and t7-fz connectivity are implicated in prosthetic hand control and can be optimized through gaze training. *Journal of NeuroEngineering and Rehabilitation*, 16(1). doi:10.1186/s12984-019-0524-x.
- Petrini, F., Mazzoni, A., Rigosa, J., Giambattistelli, F., Granata, G., Barra, B., Pampaloni, A., Guglielmelli, E., Zollo, L., Capogrosso, M., Micera, S., and Raspopovic, S. (2019). Microneurography as a tool to develop decoding algorithms for peripheral neuro-controlled hand prostheses. *BioMedical Engineering OnLine*, 18. doi:10.1186/s12938-019-0659-9.
- Řezanková, H. (2018). Different approaches to the silhouette coefficient calculation in cluster evaluation. In *21st International Scientific Conference AMSE Applications of Mathematics and Statistics in Economics 2018*, 1–10.
- Roux, F.E., Djidjeli, I., and Durand, J.B. (2018). Functional architecture of the somatosensory homunculus detected by electrostimulation. *The Journal of Physiology*, 596(5), 941–956. doi:10.1113/jp275243.
- Schalk, G., McFarland, D., Hinterberger, T., Birbaumer, N., and Wolpaw, J. (2004). BCI2000: A general-purpose brain-computer interface (BCI) system. *IEEE Transactions on Biomedical Engineering*, 51(6), 1034–1043. doi:10.1109/tbme.2004.827072.
- Sinaga, K.P. and Yang, M.S. (2020). Unsupervised k-means clustering algorithm. *IEEE Access*, 8, 80716–80727. doi:10.1109/ACCESS.2020.2988796.
- Svozil, D., Kvasnicka, V., and Pospíchal, J. (1997). Introduction to multi-layer feed-forward neural networks. *Chemometrics and Intelligent Laboratory Systems*, 39, 43–62.
- Zaki, M.J. and Meira, W. (2014). *Data Mining and Analysis: Fundamental Concepts and Algorithms*. Cambridge University Press, USA.
- Zhang, T., Jiang, L., and Liu, H. (2018). Design and functional evaluation of a dexterous myoelectric hand prosthesis with biomimetic tactile sensor. *IEEE Transactions on Neural Systems and Rehabilitation Engineering*, 26(7), 1391–1399. doi:10.1109/TNSRE.2018.2844807.
- Zilles, K. (2018). Brodmann: a pioneer of human brain mapping—his impact on concepts of cortical organization. *Brain*, 141(11), 3262–3278. doi:10.1093/brain/awy273.